Auxin involvement in tepal senescence and abscission in *Lilium*: a tale of two lilies

Lara Lombardi[a], Laia Arrom[b,e], Lorenzo Mariotti[a], Riccardo Battelli[c], Piero Picciarelli[c], Peter Kille[e], Tony Stead[d], Sergi Munne Bosch[b], Hilary Rogers[e*]

[a]Department of Biology, University of Pisa, Via Ghini 5, 56126 Pisa, Italy.

[b]Department of Plant Biology, Faculty of Biology, University of Barcelona, Avinguda Diagonal, 645, 08028 Barcelona, Spain

[c]Department of Agriculture, Food and Environment, University of Pisa, Via Mariscoglio 34, 56124, Italy

[d]School of Biological Sciences, Royal Holloway, University of London, Egham Hill, Egham, TW20 0EX, UK.

[e]School of Biosciences, Cardiff University, Main Building, Park Place, Cardiff CF10 3AT, UK.

***corresponding author:**

Email rogershj@cf.ac.uk
Tel +44(0)2920876352
Fax+44(0)2920874305

Author email addresses:

Lara Lombardi	lara.lombardi@.unipi.it
Laia Arrom	laia.arromasc@gmail.com
Lorenzo Mariotti	lmariotti@biologia.unipi.it
Riccardo Battelli	riccardobattelli@gmail.com
Piero Picciarelli	piero.picciarelli@unipi.it
Peter Kille	kille@cf.ac.uk
Tony Stead	A.Stead@rhul.ac.uk
Sergi Munné-Bosch	smunne@ub.edu

Date of submission: 03/09/14
No. of tables and figures: 2 Tables; 6 Figures
Supplementary data: 2 Tables; 3 Figures
Total word count: 8075

Short running title: Auxin involvement in tepal senescence and abscission in *Lilium*

30 word statement:

Strong evidence is presented for auxin regulating lily tepal abscission timing in relation to senescence; transcriptome data is used to correlate auxin levels with expression of auxin-related genes.

(28 words)

ABSTRACT

Petal wilting and/or abscission terminates the life of the flower. However, how wilting and abscission are coordinated is not fully understood. There is wide variation in the extent to which petals wilt before abscission, even between cultivars of the same species. For example tepals of *Lilium longiflorum* wilt substantially while those of the closely related *Lilium longiflorum* x Asiatic hybrid (L.A.) abscise turgid. Furthermore, close comparison of petal death in these two *Lilium* genotypes shows that there is a dramatic fall in FW/DW accompanied by a sharp increase in ion leakage in late senescent *L. longiflorum* tepals neither of which occur in *Lilium* L.A. Despite these differences, a putative abscission zone was identified in both lilies, but whilst the detachment force reduced to zero in *Lilium* L.A., wilting of the fused tepals in *L. longiflorum* occurred before abscission was complete. Abscission is often negatively regulated by auxin and the possible role of auxin in regulating tepal abscission relative to wilting was tested in the two lilies. There was a dramatic increase in auxin levels with senescence in *L. longiflorum* but not in *Lilium* L.A. Fifty auxin-related genes were expressed in early senescent *L. longiflorum* including twelve ARF-related genes. In Arabidopsis several ARF genes are involved in the regulation of abscission. Expression of a homologous transcript to Arabidopsis *ARF7/19* was 8-fold higher during senescence in *L. longiflorum* compared to abscising *Lilium* L.A. suggesting a conserved role for auxin-regulated abscission in monocotyledonous ethylene-insensitive flowers.

(242 words)

Key words: abscission zone; ARF transcription factors; floral senescence; IAA; *Lilium longiflorum*; transcriptome

INTRODUCTION

Floral life-span is tightly regulated and species-specific (Rogers, 2013). The ecological function of petals is in attracting pollinators, hence petal lifespan is often tightly linked to pollination (van Doorn, 1997). However, even in the absence of pollination, petals have a limited life-span that is terminated either by wilting or abscission. This can be further sub-divided into species where petals are abscised fully turgid and those in which some wilting occurs first. In monocotyledonous plants petals (or tepals) usually show some signs of wilting (McKenzie and Lovell, 1992; van Doorn and Stead, 1997) This ranges from *Hemerocallis* (daylily) in which 66% of dry weight (DW) is lost (Lay-Yee, 1992) to *Alstroemeria* where only 20% is lost (Chanasut *et al.*, 2003). In many species petal senescence is coordinated by the growth regulator ethylene; ethylene biosynthesis increases dramatically during petal senescence, and exposure to exogenous ethylene accelerates the process (van Doorn, 2001). However in an important group of flowers including the lilies, ethylene does not appear to play a major role in petal senescence (Rogers, 2013). A number of other plant growth regulators have been implicated in the regulation of floral senescence in ethylene insensitive species (Arrom and Munné-Bosch, 2012a). In particular auxin and cytokinin levels rose in *Lilium* L.A. var. 'Courier' prior to anthesis falling thereafter (Arrom and Munné-Bosch, 2012a). Consistent with this, treatment of *Iris* cut flowers with cytokinins increased vase life slightly (Van der Kop *et al*., 2003) as did treatment of *Narcissus* (Hunter *et al*., 2004) with GA_3.

Abscission is a well-characterised developmental process, occurring in leaves, fruit and floral organs. In cut flowers it is an important factor in their post-harvest quality (van Doorn and Stead, 1997). In all abscising tissues studied, the process can be divided into four stages (Niederhuth *et al*., 2013). The first stage involves the formation of an abscission zone (AZ) composed of a variable number of layers of small, cytoplasmically dense, cells. The structure of the AZ varies between species but is consistent within a single species (Taylor and Whitelaw, 2001). The timing of AZ formation also varies between species: for example in tomato (Malayer and Guard, 1964) and Arabidopsis (Cai and Lashbrook, 2008) it forms long before abscission while in cotton the AZ is formed only just before the organ is shed (Bornman *et al*., 1967). Once formed, the AZ is competent to respond to abscission signals initiating the second stage of abscission. In flowers these are only normally activated during senescence of the organ. However in ethylene-sensitive flowers such

as geranium application of exogenous ethylene can result in very rapid petal abscission within 1-2 hrs (Eversen *et al*., 1993). This activation of the pre-formed AZ results in the third stage of abscission: specific degradation of middle lamellae between the AZ cells by the action of a suite of hydrolytic enzymes including polygalacturonases, cellulases and endoglucanases (Roberts *et al*., 2002). This allows the AZ cells to separate and the organ to abscise (Rogers and Stead, 2011). In the fourth stage, post-abscission, a protective layer forms over the site of abscission.

Auxin was identified as a key negative regulator of floral abscission over 50 years ago (Jacobs 1962). This was demonstrated recently by manipulating auxin levels in AZ cells through the activation of bacterial auxin biosynthetic genes *iaaL* and *iaaM* specifically in these cells (Basu *et al*., 2013). However levels of auxin are also modulated by the balance between the free, active form and conjugated inactive storage form (Ludwig-Müller, 2011). It was postulated that an influx of auxin into the AZ prevents abscission from taking place (Taylor and Whitelaw, 2001) making auxin a key regulator in the final decision to abscise. Auxin is synthesised in young tissues, and in Arabidopsis petals there is a transient increase in auxin levels in buds (Aloni et al., 2006). The auxin is transported to other parts of the plant via a chemiosmotic mechanism mediated by PIN efflux carriers that determine the direction of flux (Leyser, 2006). In the leaf, it is generally accepted that the maintenance of constant polar IAA flux through the AZ prevents abscission (Osborne and Morgan, 1989; Roberts *et al*., 2002, Taylor and Whitelaw, 2001). Polar auxin transport (PAT) inhibitors, such as 1-N-naphthylphthalamic acid (NPA), provide useful tools for analyzing the importance of auxin transport during developmental processes (Nemhauser *et al*., 2000). The mode of action of NPA has not been not fully elucidated, but AtAPP1, encoding a plasma-membrane metalloprotease, has been identified as a protein with a high affinity for NPA and a likely role in processing of PIN1 efflux carriers on the plasma membrane (Murphy *et al*., 2002).

In Arabidopsis, cell wall dissolution is modulated by auxin through the action of members of the Auxin Response Factor (ARF) transcription factor family. ARF proteins are required for an auxin response: they bind to cis-elements in promoters of auxin responsive genes resulting in their activation or repression (Ulmasov *et al*., 1997). In Arabidopsis there are 23 *ARF* genes (Wang *et al*., 2007) and four of them have a role in organ abscission. *ARF1*, *ARF7* and *ARF19* are directly up-regulated by auxin, these in turn up regulate *ARF2* which acts to inhibit the expression of the

hydrolytic enzymes (Ellis *et al.*, 2005) responsible for middle lamella breakdown. In rice there are 25 ARF genes; OsARF7 and OsARF9 show the closest homology to AtARF1, OsARF16 shows closest homology to AtARF7 and AtARF9 while OsARF4 is the closest homologue to AtARF2 (Wang *et al.*, 2007).

Lilium species include commercially important cut flowers especially as hybrids (Benschop *et al*., 2010). The first group of hybrids produced were the Asiatic hybrids derived from species native to central and East Asia. These have been further crossed to *Lilium longiflorum* to produce *Lilium* L.A. (*L. longiflorum* x Asiatic) hybrids. Lily hybrids include both abscising and non-abscising cultivars (van Doorn, 2001) although most cultivars show some wilting, with a longer time between wilting and tepal fall in Asiatic cultivars. The senescence patterns of both *Lilium longiflorum* (Battelli *et al*., 2011) and the *Lilium* L.A. hybrid var 'Courier' (Arrom and Munné-Bosch, 2010, 2012a,b) have been recently studied. Tepals of *L. longiflorum* wilt substantially during senescence but remain attached, whereas tepals of *Lilium* L.A abscise following less severe wilting. This offers the opportunity to compare the senescence process in these two closely related genotypes. Specifically the aim of this work was to test to what extent paradigms for the role of auxin in abscission, and up-regulation of *ARF* genes developed with model species such as Arabidopsis can be applied to this taxonomically divergent, ethylene-insensitive genus.

MATERIALS AND METHODS

Plant material

Lilium longiflorum cv. 'White Heaven' was grown in a commercial greenhouse and *Lilium* L.A. var.'Courier' (*L. longiflorum* x Asiatic hybrid) plants were obtained from greenhouse-grown bulbs. Individual flowers were harvested at the stage of closed bud by cutting above the last leaf. Flowers were placed in distilled water and kept in a growth chamber at 22°C and 50% relative humidity. Under the conditions used, flower development and senescence progressed in a very predictable way from closed bud to full senescence (*L. longiflorum*) or abscission (*Lilium* L.A.).

Samples were collected from comparable developmental stages for the two species: closed flowers (CB), full bloom flowers at anthesis (FB), flowers showing the first visible signs of senescence on outer tepals (ES) and flowers at the end of their vase life (FS), which was full dryness and wilting for *L. longiflorum* and abscission for

Lilium L.A. Where appropriate, flowers were harvested also one or two days after either ES or FS.

Exogenous treatments with IAA and NPA

Flowers at the stage of closed bud (CB) were treated with 10 µM IAA or with 50 µM 1-N-naphthylphthalamic acid (NPA), to inhibit auxin transport added to the water in which the stems were immersed. Both treatments were applied throughout the experiment from closed bud to full senescence. Only outer tepals were sampled for all the analyses.

Ion leakage

Discs (8 mm diameter) were cut from each side of the central vein of the outer tepals about half-way from the tip (20 discs per tepal) and placed in 10 ml distilled water in Petri dishes. After a 2 h wash to remove ions from cut surfaces, the water was aspirated and fresh distilled water was added. Following incubation for 6h, conductivity of the bathing solution (sample conductivity) was measured with a conductivity meter (HI-8733, HANNA Instruments). Fresh distilled water (10 ml) was then added to the tepal discs and boiled for 15 min. After cooling to room temperature, conductivity was measured again to obtain the subtotal conductivity.

Ion leakage was expressed as relative conductivity, which was calculated as sample conductivity divided by total conductivity (the sum of sample conductivity and subtotal conductivity).

RNA extraction and cDNA preparation

RNA was extracted from outer tepals with TRI reagent (Sigma, St Louis, MO, USA) according to the manufacturer's instructions. RNA was subjected to DNase treatment using the TURBO DNA-free kit (Ambion Inc., Austin, TX, USA) to remove contaminating genomic DNA. Two micrograms of RNA was reverse transcribed into cDNA using the High Capacity cDNA Reverse Transcription Kit (Applied Biosystems, Foster City, CA, USA) in accordance with the manufacturer's instructions.

Illumina reference transcriptome sequencing of *L .longiflorum* tepals

Total RNA was extracted from FB and ES stage *Lilium longiflorum* tepals as described above and pooled. Quality of the RNA was checked by gel electrophoresis and capillary eletrophoresis using a Bioanalyzer (RNA Nano Chip) and concentration determined using absorption spectroscopy using a Nanodrop. A cDNA library was constructed by BaseClear (www.baseclear.com) following Tru-Seq (Illumina) protocol and sequenced on Illumina Hi-Seq 2000 using a 50 cycle paired ended protocol. A reference transcriptome was assembled using CLC Genomics workbench (CLC bio). Validity of the assembly was performed by re-mapping (CLC genomic Workbench, CLC bio) the original read onto the assembly and through functional annotation, with the former also providing a relative abundance of transcripts in the original sample. Functional annotation was performed using BLASTX was used to interrogate the non-redundant protein sequence data downloaded from NCBI (01/11/2012) together with the Uniprot database (01/11/2012). Putative annotation assignment was performed at an e-value cut-off of < 1E-05. Blast results were integrated into BLAST2GO (Conesa and Gotz, 2008), which was used to generate putative gene function and ontological assignment. Transcriptome data were deposited with the Sequence Read Archive (SRA) database at NCBI, (SRA Experiment: SRX690392)

Cloning of *Lilium* L.A. aminopeptidase P1 (APP1)

Degenerate primers were designed based on sequences from an *Alstroemeria* auxin responsive gene *APP1* (Wagstaff *et al*., 2010) and similar sequences from rice, *Ricinus* and *Sorghum.* These were used to amplify a 195 bp product. This was purified using a Qiaquick kit and ligated into pGEM-TEasy (Pomega). Based on the sequence from the cloned fragment, specific primers were designed for quantitative real-time PCR (all primers are listed in Supplementary Table 1).

Quantitative RT-PCR

Specific primers (Table S1) were designed with Primer3 software (Rozen and Skaletsky, 2000) for the *Lilium* APP1, *ARF6/8, ARF 7/19* and *AUX1*-like sequences derived from degenerate PCR or contigs from the *L. longiflorum* reference tepal transcriptome. PCR products from all the primer pairs were sequenced and compared to the available sequences to verify specificity of the primers (sequences have been

deposited in the EMBL data base, accession numbers: LN606581; LN606582; LN606583; LN606584). qPCR was carried out in a 7300 real-time PCR system (Applied Biosystems) using 50 ng of cDNA and a SYBR® green PCR master mix (Applied Biosystems). The PCR product was further analysed by a dissociation curve program from 95°C to 60°C. Expression of the ribosomal 18s rRNA gene was used for internal normalization, using PUV1 and PUV2 primers which amplify a 226 bp fragment (Dempster *et al*., 1999). Data were analysed using the $2^{-\Delta\Delta CT}$ method (Livak *et al*., 2001) and presented as relative level of gene expression. All real-time qPCR reactions were run in triplicate with cDNAs synthesized from RNA extracted from three biological replicates.

IAA extraction and analysis

Frozen tepal samples from control and NPA treated flowers were homogenised in 5 vol. of cold 80% (v/v) methanol then stirred for 4 h at 4 °C, before centrifugation at 2000 xg for 15 min. The pellet was re-extracted twice; the supernatants were pooled and reduced to the aqueous phase under vacuum; pH of the supernatant was adjusted to 2.8 and partitioned 4 times against equal volumes of ethyl acetate. Samples were dried and dissolved in a small volume of 10% (v/v) aqueous acetonitrile containing 0.5% (v/v) acetic acid just before HPLC. IAA was purified by HPLC and quantified by GC–MS as previously described (Mariotti *et al.*, 2011).

Light microscopy

Abcission zones were excised from flowers at different stages of development. The pieces of tissue, approximately 1/8th of the cross sectional area, were immersed in primary fixative comprising 3% glutaraldehyde, 4% formaldehyde in 0.1 M PIPES buffer, pH 7.2 for a minimum of 1 hour. Specimens were then rinsed in 0.1M PIPES buffer, post-fixed in 1% buffered osmium tetroxide (1 hour), rinsed in buffer, block stained in 2% aqueous uranyl acetate (20 mins), dehydrated in an ethanol series and embedded in Spurr resin (Agar Scientific, Stansted, UK) in the normal way. The polymerised blocks were then reoriented in order to be able to section perpendicular to the abscission zone. Semi-thin 0.5 µm sections were cut on a Leica OMU 3 ultramicrotome and stained with 1% toluidine blue in 1% borax and photographed on a light microscope using a Nikon Coolpix 4500 digital camera.

Detachment Force

For *L. longiflorum* the free portion of the tepals were removed and the filaments and ovary trimmed further to ensure that when clamped, only the corolla tissue was held. The clamp, with attached flower, was connected to a strain gauge (Shimpo, M/no DFG-1K and the pedicel was grasped firmly and a single straight pull employed to remove the corolla. Where the corolla tore, or was pulled from the clamp, the break-strength was recorded as 'in excess of the recorded value" hence for some stages the values presented in Fig. 2 N,M are underestimates of the force to detach the corolla. For *Lilium L.A.* individual tepals were trimmed by about one third of their length, then clamped and the detachment force determined using a single straight pull of the pedicel, the process then was repeated for the remaining tepals of that flower.

RESULTS

Senescence markers show significant differences in *L. longiflorum* and *Lilium* L.A.

Although flower life progresses through similar stages in *L. longiflorum* and in *Lilium* L.A., the final destiny of the tepals diverges. In *L. longiflorum* tepals wilt substantially during senescence with visible browning and dehydration, however they remain attached to the flower. In contrast, *Lilium* L.A. tepals abscise without wilting while still relatively turgid (Fig. 1A). Tepal fresh weight (FW), dry weight (DW), ion leakage and protein content were compared between *L. longiflorum* and *Lilium* L.A. to establish firstly a benchmarking of the senescence progression between the two flowers and then to determine key differences that might be related to the different strategies of wilting versus abscission in these closely related genotypes. Early senescence (ES) is defined in both genotypes as the earliest stage showing visible signs of senescence such as tepal browning and increased translucency, while full senescence (FS) is defined in *Lilium* L.A. as the time of abscission and in *L. longiflorum* as complete wilting and full dehydration of the tepals (Fig. 1A). In both genotypes, FW/DW falls as tepals progress from closed bud through full bloom to senescence (Fig. 1B). However, in the later stages of senescence there is a marked difference. Whereas in *Lilium* L.A. tepals there is a gradual reduction in FW/DW, in *L. longiflorum* there is a sharp decline between early and late senescence stages. There is also marked difference in the pattern of ion leakage (Fig. 1C). In *Lilium* L.A. electrolyte leakage remains relatively low and constant throughout bud opening and

senescence, in *L. longiflorum* there is a sharp increase in ion leakage between early and late senescence. In contrast, the decline in protein levels follows essentially the same trend in the two genotypes, although protein levels in *L. longiflorum* are lower throughout (Fig. 1D).

An AZ forms in both *L. longiflorum* and *Lilium* L.A. but the detachment of *L. longiflorum* is anomalous

In *L. longiflorum* outer tepals and inner tepals are fused over the lower third of the tepal length. with the margins of the outer tepals fused to the midrib of the inner tepals. Thus in transverse section (Fig. 2 A-C) there can appear to be two whorls of tepals or, if looking even closer to the pedicel, the individual outer tepals may also overlap giving the appearance of multiple whorls of tepals. When examining the AZ in LS this results in several structures being visible, each with its own putative AZ (Fig. 2D).

In section, the AZ of each *L. longiflorum* tepal was visible. Even in freshly opened flowers at FB (Fig. 2 D), the putative AZ, comprised of a series of smaller cells, could be recognised. At higher magnification the beginnings of a fracture line was discernible running between these cells (Fig. 2E). However in older flowers, several days after FS, this fracture line had not progressed significantly (Fig. 2F). The AZ was identifiable at the base of *Lilium* L.A. tepals even in closed buds (Fig. 2G) and cell wall dissolution was visible in the AZ of those flowers approaching ES (Fig. 2H).

Detachment force was measured in both lilies to establish whether the AZs observed were fully functional. In *L. longiflorum*, small dark lines, that later developed into cracks (Fig. 3A), were visible on the outside of the tissue at the point where the AZ would be expected to be situated. The fusion of the tepals in *L. longiflorum* meant that unlike in *Lilium* L.A., only the force to detach the corolla, not individual tepals, could be quantified (Fig. 3 B,C).

In early stage buds through to freshly opened flowers the force to remove the corolla in *L. longiflorum* either exceeded 1000g (the limit of the force gauge) or more often the corolla tissue tore at approximately 700-800g, although in some fully open flowers detachment of the corolla at the AZ occurred at 500-600g (Fig. 3C) As the flowers senesced and wilted both the extent of the cracking (Fig. 3A) increased concomitant with a decrease in the force needed to detach the corolla. However in flowers with wilted, browning tepals (ie beyond FS) where the external cracks

appeared to be both extensive and deep (FS+2 in Fig. 3A), the corolla still required 100-200g force to remove the corolla (Fig. 3B) showing that the abscission process was far from complete even in senescent flowers that had passed the end of their vase life. In younger, freshly opened flowers (FB), no external cracking was visible (Fig. 3A) and the corolla could not be forcibly be removed by the strain gauge (Fig. 3B).

In *Lilium* L.A. some tepals could be detached from flowers that appeared to be at the FB stage although most tore rather than detached (Fig. 3C). By the ES stage virtually all tepals could be detached and the force needed was greatly reduced (c. 600g); by the FS stage all tepals had already abscissed but in the time between ES and FS the force needed to detach the tepals decreased as would be expected for an organ showing a typical abscission process (Fig. 3C).

Auxin levels differ between the two lilies during tepal senescence

Since auxin appears to be a key regulator of abscission, the level of total IAA as well as active free-IAA and inactive conjugated forms (ester-linked to sugars and amide-linked to amino acids and peptides) was determined for both lily genotypes. Around the time of flower opening (from CB to FB) IAA content was similar in the two lilies, at about 100-150 ng/g DW. Then, as senescence progressed, in *L. longiflorum* both free-IAA and conjugated-IAA increased dramatically (Fig.4A) although the ratio of free to conjugated IAA was essentially 1:1 throughout the flower lifespan (Fig. S1). In contrast, free-IAA levels in *Lilium* L.A. remained low at every stage, from closed bud to abscission while the portion of inactive IAA-amide gradually increased (Fig.4B). Note that in *Lilium* L.A. the ratio of free to conjugated-IAA changed from about 1:1 to 1:2 between CB and abscission (Fig. S1).

The effect of exogenous application of IAA was tested on both lily genotypes. No effect was seen either on senescence progression or timing of abscission (data not shown).

Analysis of the lily tepal transcriptome reveals 50 genes related to auxin biosynthesis and perception including 12 ARF-like genes.

Forty million reads of a *L. longiflorum* reference transcriptome from ES tepals were assembled into 13,000 unigenes. Fifty unigenes showed homology to auxin-related genes from other species (Table 1) consistent with the high levels of auxin detected. Twelve unigenes showed homology to genes belonging to the ARF family of

transcription factors, and could be assigned to six Arabidopsis homology groups: *AtARF8/6*, *AtARF9/18/11*, *AtARF 19*, *AtARF3/4 AtARF7/19* and *AtARF16*. (Table S2). Homology was assessed based on the inclusion in the contig sequence of motifs III and IV, which are consensus sequences shared by AUX/IAA proteins but are discriminatory between different ARF genes in rice (Wang *et al*., 2007) (Fig. S2). Primers were designed to two contigs with homology to *AtARF6/8*, and *AtARF7/19* (contigs 651 and 7111 respectively) and verified by PCR and sequencing of products.

The transcript level of the homologues fell with tepal age in both lilies, however with different patterns (Fig. 5A and B). In *Lilium* L.A. there was a peak in transcript level at full bloom, which then essentially disappeared at abscission; in *L. longiflorum* the highest expression was in CB and expression then declined gradually.

The transcript level of the homologue of Arabidopsis *ARF7/19* fell with development and senescence in *Lilium* L.A. while in *L. longiflorum*, which has the higher auxin content and delayed incomplete abscission, levels rose slightly during flower life and were much higher than in the *Lilium* L.A. at both early and late stages of senescence (ES and FS) (Fig. 5 C and D).

NPA has opposite effects in *L. longiflorum* and *Lilium* L.A.

When the flowers at stage CB were treated with NPA, a widely used auxin transport inhibitor, senescence progression in *L. longiflorum* and the time of abscission in *Lilium* L.A. did not change (data not shown). However, NPA induced remarkable changes in IAA concentration in the whole tepal (Fig. 4). In both genotypes the levels of free-IAA during senescence stages were reduced by more than 50%. The effect of NPA treatment on the conjugated-IAA pool differed substantially between the two genotypes. In *L. longiflorum* IAA-ester and IAA-amide were reduced to about 30% of the control during early and late senescence. In contrast, in *Lilium* L.A. IAA-amide showed a dramatic increase at the time of abscission and IAA-ester levels did not change significantly.

The overall result was that, at the last stage of flower life, NPA treatment had the opposite effect on total IAA amount in the tepal in the two genotypes. In fact, in *L. longiflorum* there was an almost 2-fold reduction in total IAA concentration, while in abscised tepals of *Lilium* L.A. total IAA actually increased slightly, mainly due to the rise in IAA-conjugates (Fig. S1). Consequently, the ratio of free- to conjugated-IAA went from 1:1 to 1:7 at the time of abscission.

To determine whether the distribution of auxin across the tepal differed between genotypes, IAA content in the different regions of the tepal was determined at full senescence stage. Free-IAA was not equally distributed along the tepal axis. In both genotypes IAA concentration was higher at the base compared to the tip (Table 2) with levels over 4-fold higher in *L. longiflorum* in each region. NPA treatment resulted in a fall in IAA concentration at the tip, a greater decrease in the middle section but a significant increase at the base of the tepal in both genotypes.

APP1 and AUX 1 gene expression

To further investigate the role of auxin transport, expression of *APP1*, involved in processing of PIN efflux carriers and *AUX1* an auxin influx transporter, was determined in the two lilies during tepal development and senescence.

Using degenerate primers designed to sequences from *Alstroemeria*, rice, *Ricinus* and *Sorghum*, a 195 bp fragment homologous to Arabidopsis *AtAPP1* was obtained from *Lilium* L.A. tepal cDNA (Fig. S3). Quantitative expression analysis showed that in both lilies *APP1* transcript levels were highest in the closed bud but then there was an opposite trend during senescence (Fig.6A and B). Expression was undetectable at abscission in *Lilium* L.A. while it was still high at the last stage of senescence in *L. longiflorum*, coincident with the highest levels of IAA (Fig. 3A).

The expression of the homologue of *AUX1*, decreased with progression of senescence in both lilies (Fig. 6C and D), although levels were almost 3 fold higher at full bloom in *Lilium* L.A. Thus early senescence in *Lilium* L.A. was accompanied by a 2-fold greater fall in expression compared to *L. longiflorum*.

DISCUSSION

Given the differences in senescence progression and final abscission between the two lily genotypes, the focus of this work was to discover whether contrasting auxin levels could explain differences in progression of abscission in relation to senescence.

Firstly a comparison was made of the senescence patterns between the two genotypes: *Lilium longiflorum*, where petals remain attached and wilt, and *Lilium* L.A. where tepals abscise turgid. Visual similarities between the developmental stages from closed bud to early senescence, were supported by measurements of FW/DW and ion leakage. In both genotypes FW/DW fell gradually, and ion leakage remained constant

from CB to FB stages. However, as the flowers entered senescence their programmes diverged. Whereas in *Lilium* L.A. FW/DW continued to fall gradually, there was a sudden 2-fold drop between early and late senescence stages in *L. longiflorum*. This was accompanied by a doubling in ion leakage. These parameters are indicative of a rapid increase in water loss and cell death in *L. longiflorum* as senescence progresses but not in *Lilium* L.A. This is common in many species, including other lilies such as *Hemerocallis* (Lay-Yee *et al*., 1992), where there is substantial weight loss during senescence. In *Alstroemeria*, as in *L. longiflorum*, ion leakage rose sharply coincident with the first signs of visual senescence (Leverentz *et al*., 2002). The lack of increases in the rate of weight loss and ion leakage in *Lilium* L.A. are reminiscent of other species such as tulip where fresh weight fell to only about 70% of its maximal value (Azad et. al., 2008), and *P. yedoensis* petals where no signs of PCD were detected prior to turgid abscission (Yamada *et al*., 2007). Thus not only do *Lilium* L.A. tepals abscise but they do so in a relatively intact state, suggesting a very different senescence programme to *L. longiflorum*.

One possibility for the lack of abscission in *L. longiflorum* would be the failure to develop an AZ at all (Rogers and Stead, 2011). However examination of the base of the outer tepals of both genotypes revealed that there is what appears to be a functional AZ in both,. This suggests that the failure to completely abscise *L. longiflorum* tepals must depend on the signals that control the timing and completion of abscission. Differences in auxin levels in the AZ are a key component in tipping the balance towards abscission (Taylor and Whitelaw, 2001). Therefore levels of auxin were compared throughout development and senescence across whole tepals of the two lilies. The dramatic increase in auxin levels in late senescence in *L. longiflorum* tepals would be consistent with a role for this growth regulator in delaying activation and/or completion of the AZ while senescence processes such as cell death and water loss are still progressing in other cells or tissues. The constant and low levels of auxin in *Lilium* L.A. are consistent with an earlier activation and completion of the AZ, allowing tepals to abscise turgid. Since the balance between free and conjugated auxin is also important in determining the activity of this growth regulator (Rosquete *et al*., 2012), the finding that at full senescence *L. longiflorum* tepals contained higher levels of free compared to the two inactive conjugated forms further indicates that the auxin is active in this tissue. In contrast in *Lilium* L.A. tepals

there was substantially more IAA-amide at full senescence than free-IAA indicating that as well as lower levels of auxin, more of it was also conjugated and therefore inactive. This suggests several possible regulatory methods: an increased biosynthesis or transport, or reduced metabolism of the auxin as well as differences in the activity of enzymes regulating the balance between conjugated IAA and free IAA.

To further understand the role of auxin in these lilies, auxin-related genes were derived from an early senescent tepal reference transcriptome. Target sequences for lily ARF genes known in Arabidopsis to be important in regulating abscission were found: specifically Arabidopsis *ARF1, ARF7/19* and *ARF2*. No homologues to *ARF1* or *ARF2* were obtained despite a good depth of sequencing. This could be due to low levels of expression at this stage of development: in Arabidopsis, *ARF1* is expressed at very low levels during petal and leaf senescence, *ARF2* is up-regulated in senescent leaves but not in older petals (eFP browser; Winter *et al*., 2007). However putative homologues of *ARF7/19* were identified and their expression pattern in *L. longiflorum* during senescence is consistent with up-regulation of the expression of these genes in Arabidopsis older petals. In Arabidopsis *ARF19* is induced by auxin (Wilmoth *et al*., 2005) and is part of a positive feedback loop involving *ARF7*. Thus the up-regulation of the lily *ARF7/19*-like gene is also consistent with an increase in auxin in this genotype. In contrast the fall in expression of the *ARF7/19*-like gene with senescence in *Lilium* L.A. is consistent with the slight fall in free auxin in this genotype and also with the completion of abscission. As a comparison the expression of *ARF6/8* was also analysed and found to be down-regulated during senescence in both lily genotypes. In Arabidopsis *ARF8* is involved in petal growth and expansion (Varaud *et al*., 2011) and both *ARF6* and *ARF8* are strongly expressed in both young and older petals but their expression declines with petal age.

Having established a clear correlation between auxin levels and abscission timing in the two lily genotypes we also asked if auxin transport was involved since this may be more important that absolute concentration of IAA. NPA treatment did not affect timing of senescence in *L. longiflorum* or abscission in *Lilium* L.A. This is in contrast to leaf abscission in *Mirabilis jalapa* where treatment with NPA delayed ethylene-induced abscission (Meir *et al*., 2006). However effects of NPA on senescence are consistent with those seen in Iris, another ethylene-insensitive flower (van Doorn *et al*., 2013). Nevertheless NPA did affect IAA levels differentially in the two

genotypes, especially the levels of conjugated IAA suggesting that auxin transport is required for determining levels of free auxin. The fall in expression of *APP1* in *Lilium* L.A. during senescence, but not in *L. longiflorum,* may suggest that auxin efflux is a factor in maintaining high levels of auxin in the latter. The distribution of auxin levels from base to tip of the petal fits with previous data showing higher levels at the base and is consistent with auxin transport in the petal during development. The effect of NPA suggests that the auxin transport is still active and is in the direction of base to tip since NPA treatment reduces auxin levels in the middle and tip sections and increases free auxin concentration at the base. The increase in auxin at the base with NPA treatment suggests a blockage of auxin transport due to the inhibitory effect of the NPA. This is probably into the base of the tepal from other floral organs, since during late tepal development and senescence levels of auxin biosynthesis in the tepal itself are likely to be low (Aloni *et al.*, 2006). However, since this affects both lilies, the conclusion is that while auxin levels correlate with timing of abscission, transport of auxin does not.

Conclusions

Despite their close genetic relationship *L. longiflorum* and *Lilium* L.A. tepals age through different mechanisms indicating that wilting and abscission strategies can differ in very closely related genotypes. The presence of a fully formed AZ in both genotypes suggests that the difference in abscission relates to the very last steps of AZ activation/completion. There is a clear correlation between auxin levels and abscission timing in relation to senescence markers. Furthermore the role of auxin in abscission previously elucidated in *Arabidopsis* may involve the same mechanism through the ARF genes in this taxonomically unrelated group. Auxin transport does not affect senescence and effects of the auxin transport inhibitor NPA did not affect the two genotypes differentially indicating that although differing auxin levels may be responsible for the timing of tepal abscission this is not due to differences in auxin transport during senescence.

Acknowledgments

We would like to thank Lizzie Angus and Anton Page for their help with the microscopy at the Bioimaging Unit, Southampton, NHS Trust and Steve Turner for handling samples for sequencing at Cardiff School of Biosciences.

Supplementary Data

Supplementary Table S1: All primers used for PCR.

Supplementary Table S2: *L. longiflorum* contigs showing homology to ARF genes

Supp. Fig. S1: Total auxin levels as the sum of free and conjugated IAA.

Supp. Fig. S2: Alignment of *ARF*-like lily sequences with nearest rice ORF match based on BlastX homology.

Supp. Fig. S3: Alignment of *APP1*-like lily sequence with Arabidopsis *AtAPP1* gene (AT4G36760).

REFERENCES

Aloni R, Aloni E, Langhans M, Ullrich CI. 2006. Role of auxin in regulating Arabidopsis flower development. Planta **223**, 315–328.

Arrom L, Munné-Bosch S. 2010. Tocopherol composition in flower organs of *Lilium* and its variations during natural and artificial senescence. Plant Science **179**, 289-295.

Arrom L, Munné-Bosch S. 2012a. Hormonal changes during flower development in floral tissues of *Lilium.* Planta **236**, 343–354.

Arrom L, Munné-Bosch S. 2012b. Sucrose accelerates flower opening and delays senescence through a hormonal effect in cut lily flowers. Plant Science **188-189**, 41-47.

Azad AK, Ishikawa T, Sawa Y, Shibata H. 2008. Intracellular energy depletion triggers programmed cell death during petal senescence in tulip. Journal of Experimental Botany **59**, 2085-2095.

Basu MM, González-Carranza ZH, Azam-Ali S, Tang S, Shahid AA, Roberts JA. 2013. The manipulation of auxin in the abscission zone cells of Arabidopsis flowers reveals that indoleacetic acid signaling is a prerequisite for organ shedding. Plant Physiology **162**, 96-106.

Battelli R, Lombardi L, Rogers HJ, Picciarelli P, Lorenzi R, Ceccarelli N. 2011. Changes in ultrastructure, protease and caspase-like activities during flower senescence in *Lilium longiflorum.* Plant Science **180**, 716-725.

Benschop M, Kamenetsky R, Le Nard M, Okubo H, De Hertogh, A. 2010. The global flower bulb industry: production, utilization, research. Horticultural Reviews **36**, 1.

Bornman CH, Spurr AR, Addicott FT. 1967. Abscisin, auxin, and gibberellin effects on the developmental aspects of abscission in cotton (*Gossypium hirsutum*). American Journal of Botany **54**, 125-135.

Cai S, Lashbrook CC. 2008. Stamen abscission zone transcriptome profiling reveals new candidates for abscission control: enhanced retention of floral organs in transgenic plants overexpressing *Arabidopsis ZINC FINGER PROTEIN2*. Plant Physiology **146**, 1305-1321.

Chanasut U, Rogers H, Leverentz M, Griffiths G, Thomas B, Wagstaff C, Stead, A. 2003. Increasing flower longevity in Alstroemeria. Postharvest Biology and Technology **29**, 325-333.

Conesa A, Götz S. 2008. Blast2GO: A comprehensive suite for functional analysis in plant genomics. International Journal of Plant Genomics **2008**, 1-12.

Davies RT, Goetz DH, Lasswell J, Anderson MN, Bartel B. 1999. *IAR3* encodes an auxin conjugate hydrolase from *Arabidopsis*. Plant Cell **11**, 365-376.

Dempster EL, Pryor KV, Francis D, Young JE, Rogers HJ. 1999. Rapid DNA extraction from ferns for PCR-based analyses. BioTechniques **27**, 66-68.

Ellis CM, Nagpal P, Young JC, Hagen G, Guilfoyle TJ, Reed JW. 2005. *AUXIN RESPONSE FACTOR1* and *AUXIN RESPONSE FACTOR2* regulate senescence and floral organ abscission in *Arabidopsis thaliana*. Development **132**, 4563-4574.

Eversen KB, Clark DG, Singh A. 1993. Rapid ethylene-induced gene expression during petal abscission. In: Pech JC, Latche A, Balague C, eds. *Cellular, molecular aspects of the plant hormone ethylene*. Dordrecht, The Netherlands: Kluwer Academic Publishers, 278–283.

Hunter DA, Ferrante A, Vernieri P, Reid MS. 2004. Role of abscisic acid in perianth senescence of daffodil (*Narcissus pseudonarcissus* 'Dutch Master'). Physiologia Plantarum **121**, 313-321.

Jacobs WP. 1962. Longevity of plant organs: internal factors controlling abscission. Annual Review of Plant Physiology **13**, 403-436.

Lay-Yee M, Stead AD, Reid MS. 1992. Flower senescence in daylily (*Hemerocallis*). Physiologia Plantarum **86**, 308-314.

Leverentz MK, Wagstaff C, Rogers HJ, Stead AD, Chanasut U, Silkowski H, Thomas B, Weichert H, Feussner I, Griffiths G. 2002. Characterization of a novel lipoxygenase-independent senescence mechanism in *Alstroemeria peruviana* floral tissue. Plant Physiology **130**, 273-283.

Leyser O. 2006. Dynamic integration of auxin transport and signalling. Current Biology **16**, R424–R433.

Livak K, Schmittgen T. 2001. Analysis of relative gene expression data using real-time quantitative PCR and 2(-DeltaDelta C(T)) Method. Methods **25,** 402 – 408.

Ludwig-Müller J. 2011. Auxin conjugates: their role for plant development and in the evolution of land plants. Journal of Experimental Botany **62**, 1757-1773.

Malayer JC, Guard AT. 1964. A comparative developmental study of the mutant side-shootless and normal tomato plants. American Journal of Botany **51**, 140-143.

Mariotti L, Picciarelli P, Lombardi L, Ceccarelli N. 2011. Fruit-set and early growth in tomato are associated with increase in IAA, cytokinins and bioactive gibberellins. Journal of Plant Growth Regulation **30**, 405-415.

McKenzie RJ, Lovell PH. 1992. Flower senescence in monocotyledons: a taxonomic survey. New Zealand Journal of Crop and Horticultural Science **20**, 67-71.

Meir S, Hunter DA, Chen JC, Halaly V, Reid MS. 2006. Molecular changes occurring during acquisition of abscission competence following auxin depletion in *Mirabilis jalapa*. Plant Physiology **141**, 1604-1616.

Murphy AS, Hoogner KR, Peer WA, Taiz L. 2002. Identification, purification, and molecular cloning of n-1-naphthylphthalmic acid-binding plasma membrane-associated aminopeptidases from arabidopsis. Plant Physiology **128**, 935-950.

Niederhuth CE, Cho SK, Seitz K, Walker JC. 2013. Letting go is never easy: abscission and receptor‐like protein kinases. Journal of Integrative Plant Biology **55**, 1251-1263.

Nemhauser JL, Feldman LJ, Zambryski PC. 2000. Auxin and ETTIN in *Arabidopsis* gynoecium morphogenesis. Development **127**, 3877-3888.

Osborne DJ, Morgan PW. 1989. Abscission. Critical Reviews in Plant Sciences **8**, 103-129.

Roberts JA, Elliott KA, González-Carranza ZH. 2002. Abscission, dehiscence, and other cell separation processes. Annual Review of Plant Biology **53**, 131-158.

Rogers HJ. 2013. From models to ornamentals: how is flower senescence regulated? Plant Molecular Biology **82**, 563-574.

Rogers HJ, Stead AD. 2011. Petal abscission: falling to their death or cast out to die? In: *The Flowering Process and its Control in Plants: gene expression and hormone interaction.* Ed. Yash MW Research Signpost, Kerala India 229-258.

Rosquete RM, Barbez E, Kleine-Vehna J. 2012. Cellular auxin homeostasis: gatekeeping is housekeeping. Molecular Plant **5**, 772-786.

Rozen S, Skaletsky H. 1999. Primer3 on the WWW for general users and for biologist programmers. In *Bioinformatics methods and protocols* (pp. 365-386). Humana Press.

Taylor JE, Whitelaw CA. 2001. Signals in abscission. New Phytologist **151**, 323-339.

Ulmasov T, Hagen G, Guilfoyle TJ. 1997. ARF1, a transcription factor that binds to auxin response elements. Science **276**, 1865-1868.

van der Kop DAM, Ruys G, Dees D, van der Schoot C, de Boer AD, van Doorn WG. 2003. Expression of defender against apoptotic death (DAD-1) in *Iris* and *Dianthus* petals. Physiologia Plantarum **117**, 256-263.

van Doorn WG, Stead AD. 1997. Abscission of flowers and floral parts. Journal of Experimental Botany **48**, 821-837.

van Doorn WG, Celikel FG, Pak C, Harkema H. 2013. Delay of *Iris* flower senescence by cytokinins and jasmonates. Physiologia Plantarum **148**, 105-120.

Varaud E, Brioudes F, Szécsi J, Leroux J, Brown S, Perrot-Rechenmannand C, Bendahmane M. 2011. AUXIN RESPONSE FACTOR8 regulates *Arabidopsis* petal growth by interacting with the bHLH transcription factor BIGPETALp. Plant Cell **23**, 973-983.

Wagstaff C, Bramke I, Breeze E, Thornber S, Harrison E, Thomas B, Rogers HJ. 2010. A specific group of genes respond to cold dehydration stress in cut *Alstroemeria* flowers whereas ambient dehydration stress accelerates developmental senescence expression patterns. Journal of Experimental Botany **61**, 2905-2921.

Wang D, Pei K, Fu Y, Sun Z, Li S, Liu H, Tang K, Han B, Tao Y. 2007. Genome-wide analysis of the auxin response factors (ARF) gene family in rice (*Oryza sativa*) Gene **394**, 13-24.

Wilmoth JC, Wang S, Tiwari SB, Joshi AD, Hagen G, Guilfoyle TJ, Alonso JM, Ecker JR, Reed JW. 2005. NPH4/ARF7 and ARF19 promote leaf expansion and auxin induced lateral root formation. Plant Journal **43**, 118-130.

Winter D, Vinegar B, Nahal H, Ammar R, Wilson GV, Provart NJ. 2007. An "Electronic Fluorescent Pictograph" browser for exploring and analyzing large-scale biological data sets. PlosONE **8**, e718.

Yamada T, Ichimura K, van Doorn WG. 2007. Relationship between petal abscission and programmed cell death in *Prunus yedoensis* and *Delphinium belladonna*. Planta **226** 1195–1205.

FIGURE LEGENDS

Figure 1. Floral senescence progression in *L. longiflorum* and *Lilium* L.A. (A): Equivalent stages based on floral development and signs of visible senescence defined in Battelli *et al.* (2011) and Arrom *et al.* (2012) CB = closed bud; FB = full bloom; ES = early senescence; FS = full senescence. (B-C, *L. longiflorum* grey bars, *Lilium* L.A. white bars): Changes in fresh weight/dry weight (B) ion leakage (C); (D, *L. longiflorum* closed circles, *Lilium* L.A. open circles) protein content with senescence in outer tepals of the two genotypes. (Mean ± SE, n=20; asterisks indicate significant differences between the two genotypes at each stage as determined by Student's t-test (***P < 0.001.)

Figure 2. AZ in *L. longiflorum* and *Lilium* L.A. (A): TS across young flower of *L. longiflorum* 'White Heaven' showing the central ovary (Ov), anthers (An) and inner (I) and outer (O) tepals. The margins of the outer tepals are fused with the midrib of the inner tepals (arrows) that are shown on the outside in (B) and at higher magnification in (C). (D-F): LS through the corolla base of *L. longiflorum*, at FB (D-E) and at ES (F). (G-H): LS through the corolla base of *Lilium* L.A. at FB (G) and at ES (H).

Figure 3. Detachment of tepals in the two lily genotypes. (A): outside of the corolla base of *L. longiflorum* at FB, ES, FS and beyond. (B,C): force (g) required to remove the corolla of *L. longiflorum* (B) at each stage (the force required at CB and FB could not be determined as the corolla tissue tore) plus at 1 and 2 days following the FS stage, and *Lilium* L.A. (C) (again detachability could not be determined at CB and the value for FB was determined only from those that detached and may represent a considerable underestimate as n<10; in *Lilium* L.A by FS tepals had abscised naturally. Values are means ±SE with n≥10 unless otherwise stated.

Figure 4. Concentrations of endogenous free and conjugated IAA in outer tepals of control and NPA (50µM) treated flowers. (A) *L. longiflorum* and (B) *Lilium* L.A. at stages defined in Fig 1. (mean ± SE, n=10; asterisks indicate significant differences between the two genotypes at each stage as determined by Student's t-test (***P* < 0.05, ***P < 0.001). Control, grey bars; NPA treated, white bars.

Figure 5. **Relative expression of ARF-like genes by real time RT-PCR.** (A,B) transcript levels of *ARF6/8*-like gene; (C,D) transcript levels of *ARF7/19*-like gene in (A,C) *L. longiflorum* and (B,D) *Lilium* L.A. at stages defined in Fig 1. (mean ± SE, n=10; different letters indicate significant differences among stages as determined by one-way ANOVA).

Figure 6. Relative expression of *APP1*-like and *AUX1*-like genes by real time RT-PCR. Transcript levels in *L. longiflorum* (A,C) and in *Lilium* L.A. (B, D) at stages defined in Fig 1 (mean ± SE, n=10; different letters indicate significant differences among stages as determined by one-way ANOVA).

TABLES

Table 1: *L. longiflorum* petal unigenes showing homology to genes with auxin-related functions

Lily contig	accession code	match on nr database	e-value
651	A2YG67	Auxin response factor 17 Oryza sativa	0
1348	Q653U3	Auxin response factor 17 Oryza sativa	6E-11
1628	Q9XED8	Auxin response factor 9 Arabidopsis thaliana	3E-32
2468	Q9XED8	Auxin response factor 9 Arabidopsis thaliana	3E-83
5803	Q6YZW0	Auxin response factor 21Oryza sativa	2E-10
6507	Q9ZTX9	Auxin response factor 4 Arabidopsis thaliana	2E-28
7111	Q0D9R7	Auxin response factor 19 Oryza sativa	5E-60
8123	Q0DGS1	Auxin response factor 14 Oryza sativa	6E-16
9023	Q9ZPY6	Auxin response factor 11 Arabidopsis thaliana	3E-13
10581	Q653U3	Auxin response factor 17 Oryza sativa	3E-12
11452	Q5JK20	Auxin response factor 4 Oryza sativa	4E-25
11651	Q653H7	Auxin response factor Oryza sativa	3E-32
2713	B9G2A8	Auxin transport protein BIG Oryza sativa	0
3454	Q96247	Auxin transporter protein 1 Arabidopsis thaliana	1E-115
7797	Q9FEL6	Auxin transporter-like protein 3 Medicago truncatula	3E-83
6782	Q5SMQ9	Auxin efflux carrier component Oryza sativa	9E-12
4681	Q94BT2	Auxin-induced in root cultures Arabidopsis thaliana	2E-28
5083	Q6J163	Auxin-induced protein 5NG4 Pinus taeda	2E-23
10928	Q6J163	Auxin-induced protein 5NG4 Pinus taeda	5E-10
32	Q6J163	Auxin-induced protein 5NG4 Pinus taeda	3E-21
9356	Q6J163	Auxin-induced protein 5NG4 Pinus taeda	2E-31
4137	Q6J163	Auxin-induced protein 5NG4 Pinus taeda	9E-34
3596	Q6J163	Auxin-induced protein 5NG4 Pinus taeda	3E-35
3456	Q6J163	Auxin-induced protein 5NG4 Pinus taeda	6E-46
1865	Q6J163	Auxin-induced protein 5NG4 Pinus taeda	3E-52
1341	Q6J163	Auxin-induced protein 5NG4 Pinus taeda	1E-57
5697	Q6J163	Auxin-induced protein 5NG4 Pinus taeda	1E-77
7896	P33083	Auxin-induced protein 6B Glycine max	3E-09
5806	P40691	Auxin-induced protein PCNT115 Nicotiana tabacum	3E-20
1364	P40691	Auxin-induced protein PCNT115 Nicotiana tabacum	6E-65
949	Q05349	Auxin-repressed 12.5 kDa protein Fragaria ananassa	2E-16
7600	Q5VRD1	Auxin-responsive protein IAA1 Oryza sativa	8E-21
2243	Q5VRD1	Auxin-responsive protein IAA1 Oryza sativa	5E-43
4986	Q6AT10	Auxin-responsive protein IAA15 Oryza sativa	2E-17
2817	Q5Z749	Auxin-responsive protein IAA21 Oryza sativa	2E-33
3836	Q9ZSY8	Auxin-responsive protein IAA27Arabidopsis thaliana	9E-33
8767	P0C132	Auxin-responsive protein IAA30 Oryza sativa	5E-10
3951	P0C132	Auxin-responsive protein IAA30 Oryza sativa	1E-42
1293	Q6H543	Auxin-responsive protein IAA7 Oryza sativa	4E-21
3646	P32295	IAA-induced protein ARG7 Vigna radiata	0.000002
5808	P32295	IAA -induced protein ARG7 Vigna radiata	7E-07
2930	P32295	IAA -induced protein ARG7 Vigna radiata	3E-09
2438	Q67UL3	Probable auxin efflux carrier component 1c Oryza sativa	5E-82
3338	Q9LW29	AUXIN SIGNALING F-BOX 2 Arabidopsis thaliana	0.000006
9124	Q9LW29	AUXIN SIGNALING F-BOX 2 Arabidopsis thaliana	0.000009
12877	Q9LW29	AUXIN SIGNALING F-BOX 2 Arabidopsis thaliana	2E-11
11286	Q9LW29	AUXIN SIGNALING F-BOX 2 Arabidopsis thaliana	9E-12
1440	Q9LW29	AUXIN SIGNALING F-BOX 2 Arabidopsis thaliana	1E-171
12808	Q9LPW7	AUXIN SIGNALING F-BOX 3 Arabidopsis thaliana	5E-26
7557	Q0DKP3	Transport inhibitor response 1-like protein Oryza sativa	1E-55

Table 2: Free IAA content across petals of the two genotypes at full senescence (FS).

IAA ng/g DW	***L. Longiflorum***		***Lilium* L.A.**	
	control	**NPA**	**control**	**NPA**
Tip	341 ± 9 a	262 ± 7 b	55 ± 0.2 a	40 ± 0.8 b
Middle	612 ± 8.8 a	314 ± 4.3 b	122 ± 3.5 a	48 ± 0.01 b
Base	504 ± 3.6 a	572 ± 11 b	125 ± 1.3 a	140 ± 0.9 b

Letters indicate significant differences between control and treatment ($P<0.05$)

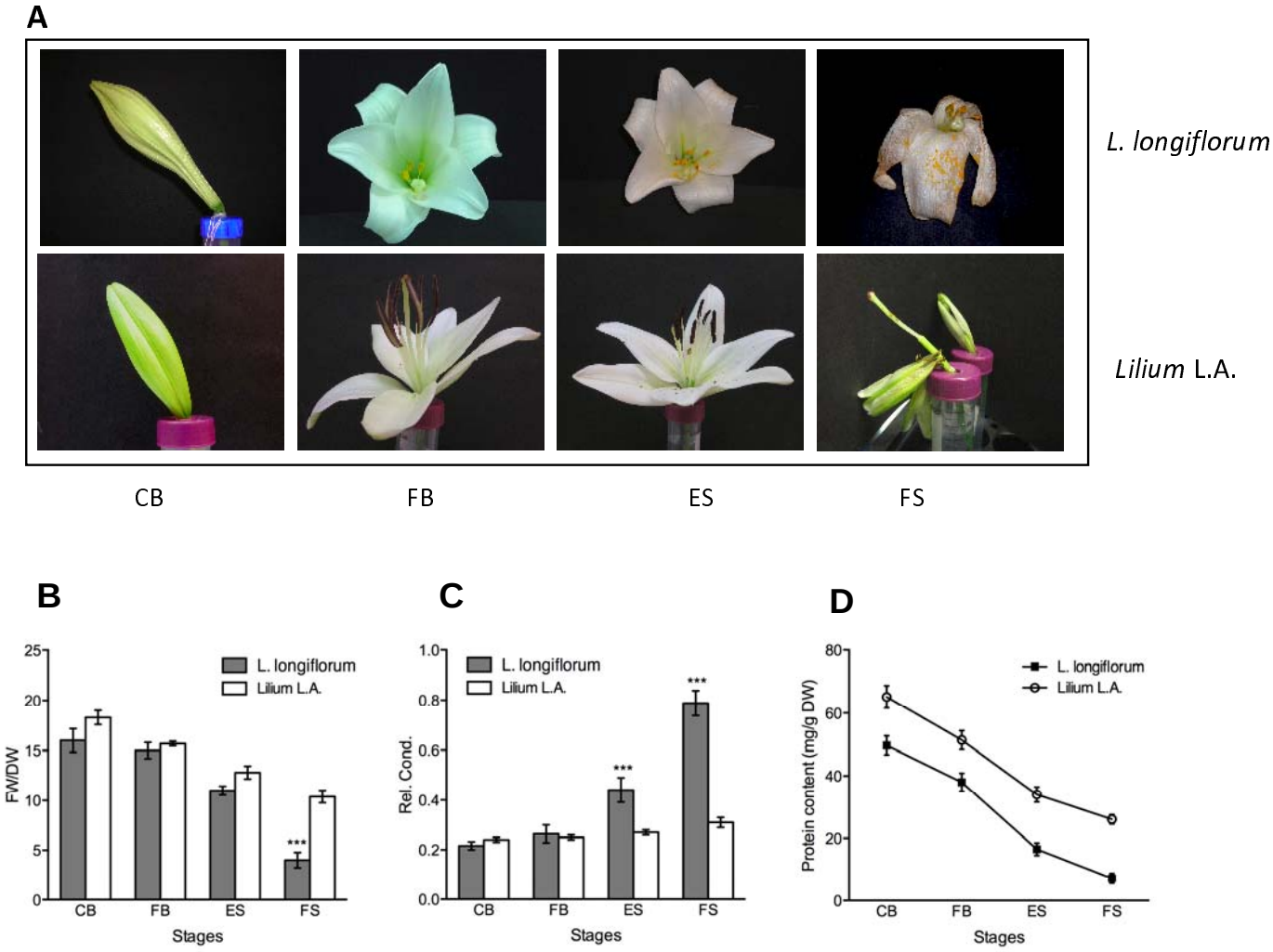

Figure 1. Floral senescence progression in *L. longiflorum* and *Lilium* L.A. (A): Equivalent stages based on floral development and signs of visible senescence defined in Battelli *et al.* (2011) and Arrom *et al.* (2012) CB = closed bud; FB = full bloom; ES = early senescence; FS = full senescence.
(B-C, *L. longiflorum* grey bars, *Lilium* L.A. white bars): Changes in fresh weight/dry weight (B) ion leakage (C); (D, *L. longiflorum* closed circles, *Lilium* L.A. open circles) protein content with senescence in outer tepals of the two genotypes. (Mean ± SE, n=20; asterisks indicate significant differences between the two genotypes at each stage as determined by Student's t-test (***P < 0.001.)

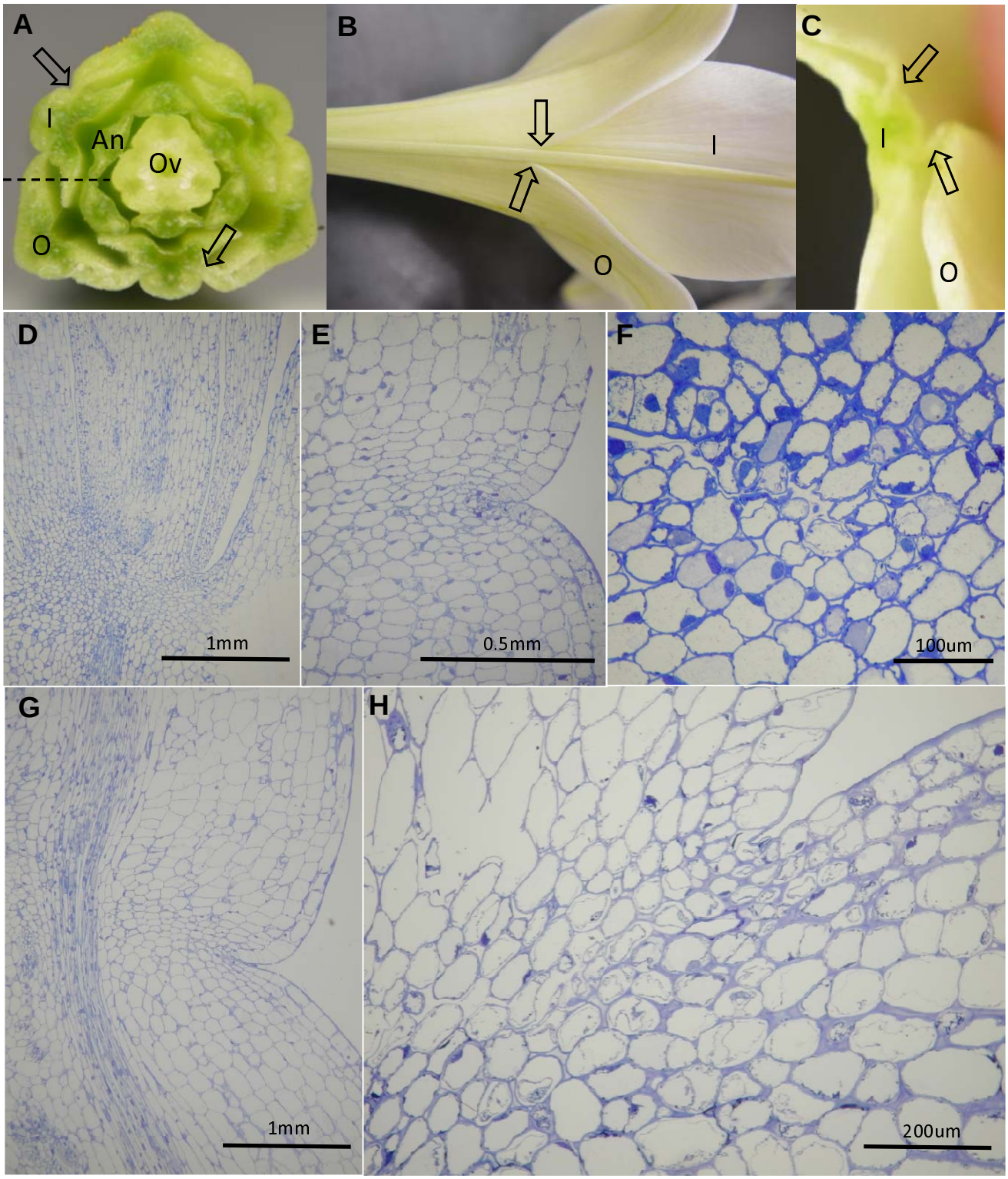

Figure 2. AZ in *L. longiflorum* and *Lilium* L.A. (A): TS across young flower of *L. longiflorum* 'White Heaven' showing the central ovary (Ov), anthers (An) and inner (I) and outer (O) tepals. The margins of the outer tepals are fused with the midrib of the inner tepals (arrows) that are shown on the outside in (B) and at higher magnification in (C). (D-F): LS through the corolla base of *L. longiflorum*, at FB (D-E) and at ES (F). (G-H): LS through the corolla base of *Lilium* L.A. at FB (G) and at ES (H).

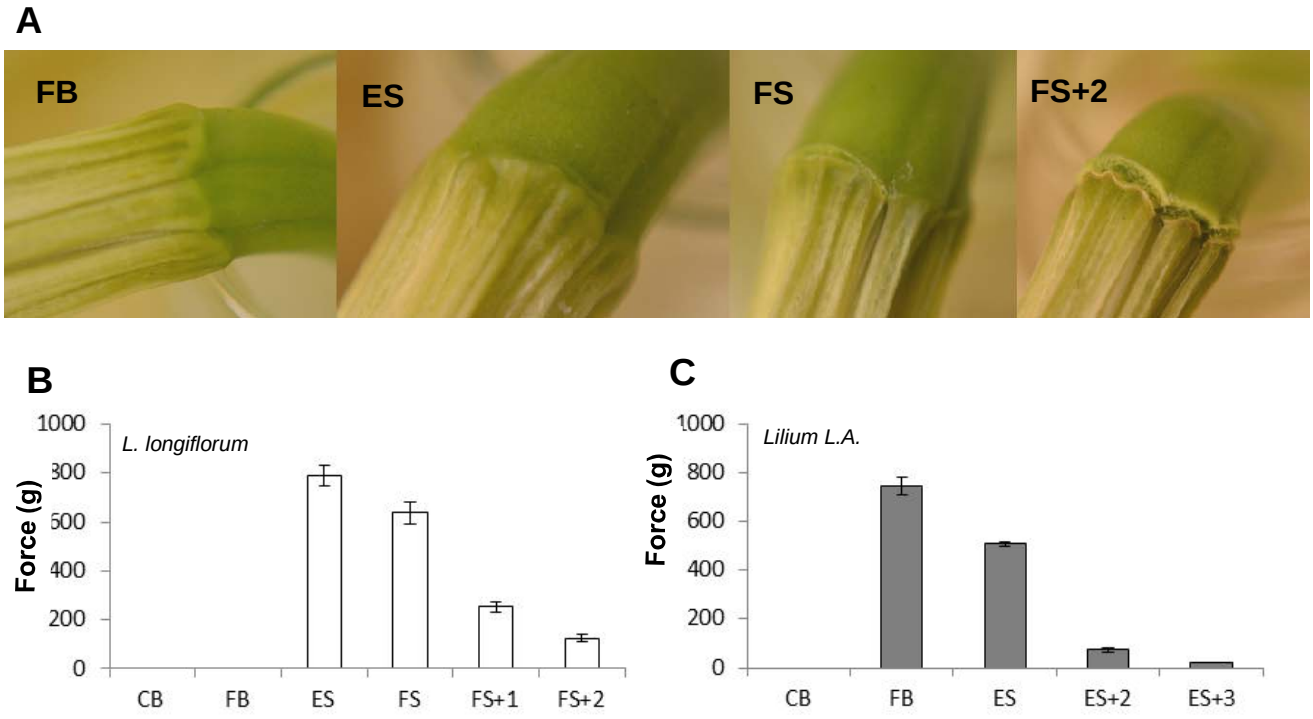

Figure 3. Detachment of tepals in the two lily genotypes. (A): outside of the corolla base of *L. longiflorum* at at FB, ES, FS and beyond. (B,C): force (g) required to remove the corolla of *L. longiflorum* (B) at each stage (the force required at CB and FB could not be determined as the corolla tissue tore) plus at 1 and 2 days following the FS stage, and *Lilium* L.A. (C) (again detachability could not be determined at CB and the value for FB was determined only from those that detached and may represent a considerable underestimate as n<10; in *Lilium* L.A by FS tepals had abscised naturally. Values are means ±SE with n≥10 unless otherwise stated.

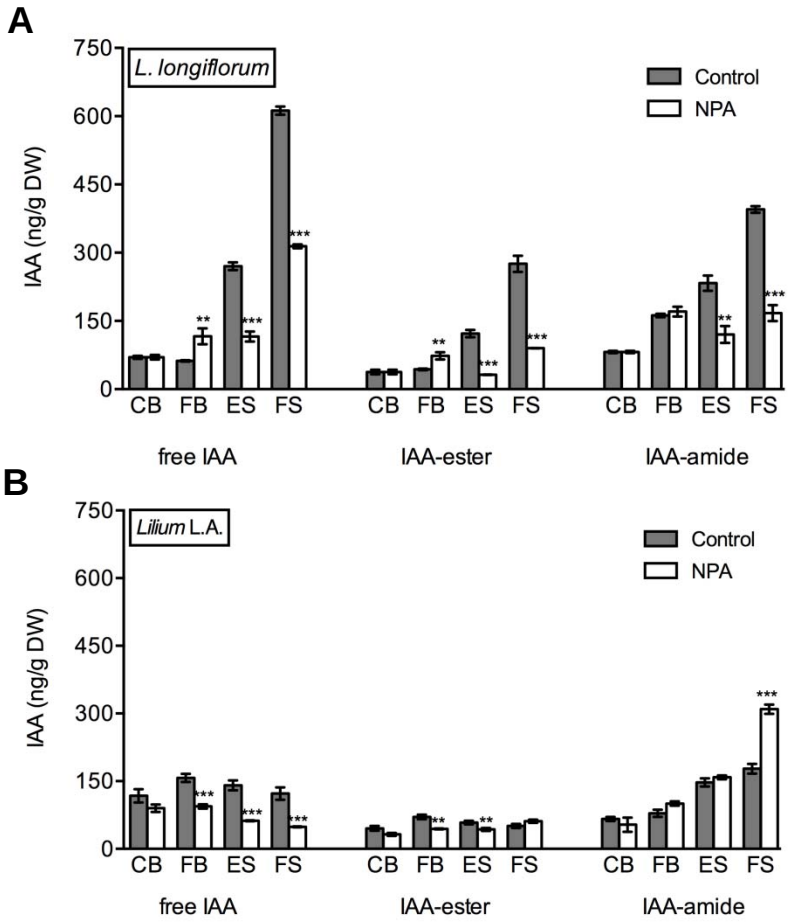

Figure 4. Concentrations of endogenous free and conjugated IAA in outer tepals of control and NPA (50µM) treated flowers. (A) *L. longiflorum* and (B) *Lilium* L.A. at stages defined in Fig 1. (mean ± SE, n=10; asterisks indicate significant differences between the two genotypes at each stage as determined by Student's t-test (***P* < 0.05, ***P < 0.001). Control, grey bars; NPA treated, white bars.

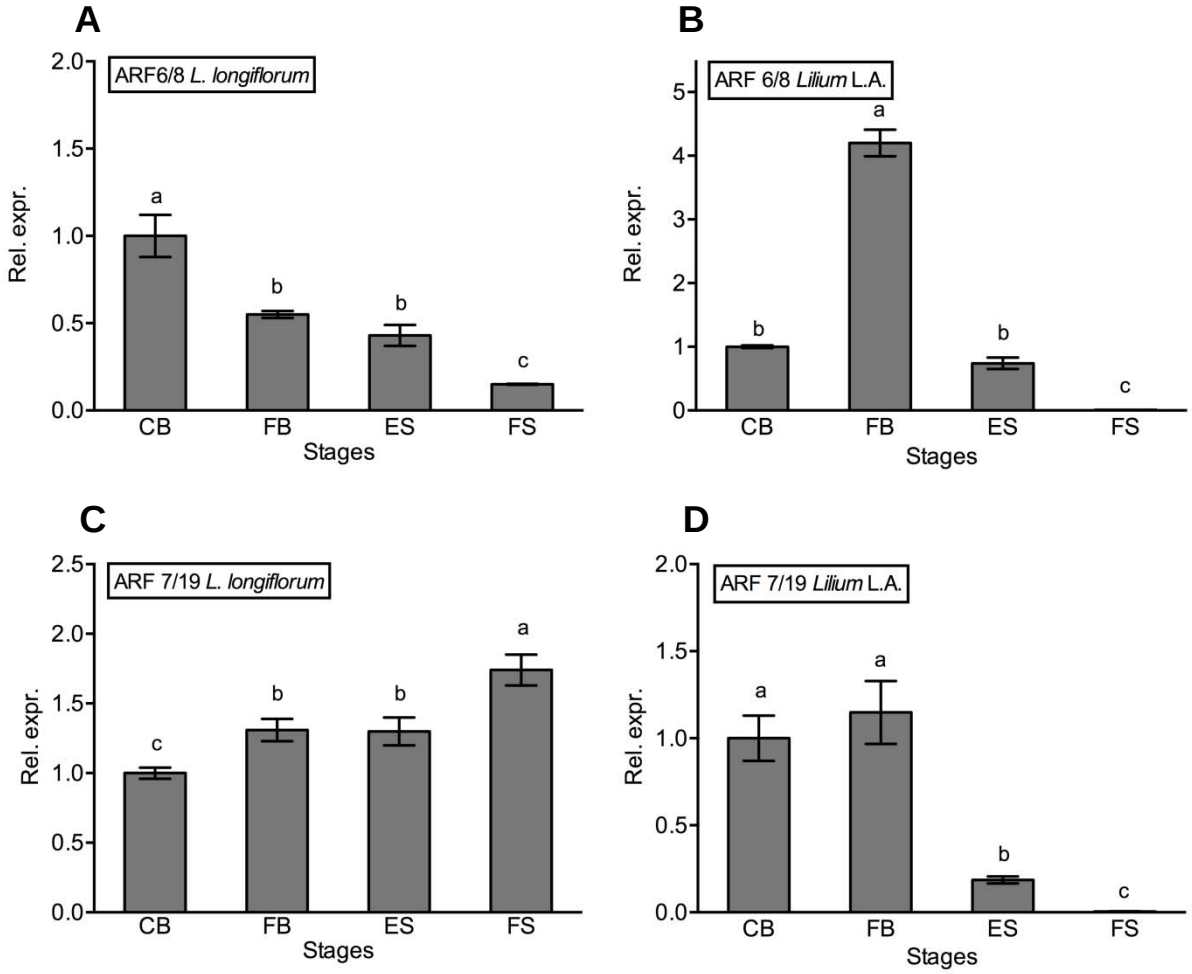

Figure 5. Relative expression of ARF-like genes by real time RT-PCR. (A,B) transcript levels of ARF6/8-like gene; (C,D) transcript levels of ARF7/19-like gene in (A,C) L. longiflorum and (B,D) Lilium L.A. at stages defined in Fig 1. (mean ± SE, n=10; different letters indicate significant differences among stages as determined by one-way ANOVA).

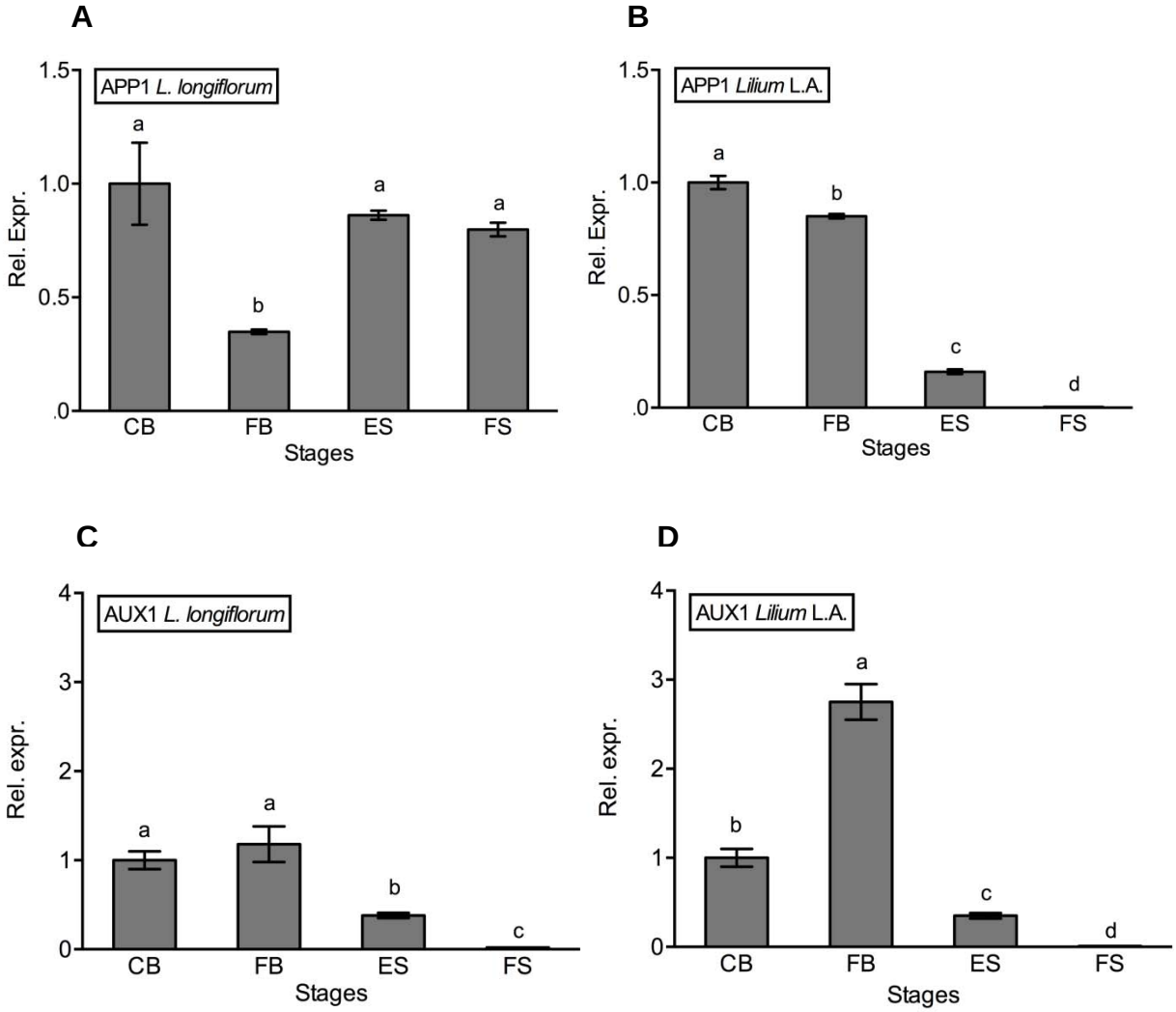

Figure 6. Relative expression of *APP1*-like and *AUX1*-like genes by real time RT-PCR. Transcript levels in *L. longiflorum* (A,C) and in *Lilium* L.A. (B, D) at stages defined in Fig 1 (mean ± SE, n=10; different letters indicate significant differences among stages as determined by one-way ANOVA).